Infectious Diseases
ACS

Article

Synthesis, Structure−Activity Relationship, and Mechanistic Studies of Aminoquinazolinones Displaying Antimycobacterial Activity

Jessica N. Akester, Paul Njaria, Aloysius Nchinda, Claire Le Manach, Alissa Myrick, Vinayak Singh, Nina Lawrence, Mathew Njoroge, Dale Taylor, Atica Moosa, Anthony J. Smith, Elizabeth J. Brooks, Anne J. Lenaerts, Gregory T. Robertson, Thomas R. Ioerger, Rudolf Mueller, and Kelly Chibale*
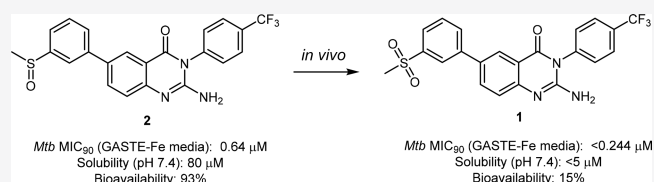
Read Online

ACCESS | Metrics & More | Article Recommendations | Supporting Information

ABSTRACT: Phenotypic whole-cell screening against *Mycobacterium tuberculosis* (*Mtb*) in glycerol−alanine−salts supplemented with Tween 80 and iron (GASTE-Fe) media led to the identification of a 2-aminoquinazolinone hit compound, sulfone **1** which was optimized for solubility by replacing the sulfone moiety with a sulfoxide **2**. The synthesis and structure−activity relationship (SAR) studies identified several compounds with potent antimycobacterial activity, which were metabolically stable and noncytotoxic. Compound **2** displayed favorable *in vitro* properties and was therefore selected for *in vivo* pharmacokinetic (PK) studies where it was found to be extensively metabolized to the sulfone **1**. Both derivatives exhibited promising PK parameters; however, when **2** was evaluated for *in vivo* efficacy in an acute TB infection mouse model, it was found to be inactive. In order to understand the *in vitro* and *in vivo* discrepancy, compound **2** was subsequently retested *in vitro* using different *Mtb* strains cultured in different media. This revealed that activity was only observed in media containing glycerol and led to the hypothesis that glycerol was not used as a primary carbon source by *Mtb* in the mouse lungs, as has previously been observed. Support for this hypothesis was provided by spontaneous-resistant mutant generation and whole genome sequencing studies, which revealed mutations mapping to glycerol metabolizing genes indicating that the 2-aminoquinazolinones kill *Mtb in vitro* via a glycerol-dependent mechanism of action.

KEYWORDS: tuberculosis, Mycobacterium tuberculosis, drug discovery, 2-aminoquinazolinones

Mtb MIC$_{90}$ (GASTE-Fe media): 0.64 μM
Solubility (pH 7.4): 80 μM
Bioavailability: 93%

Mtb MIC$_{90}$ (GASTE-Fe media): <0.244 μM
Solubility (pH 7.4): <5 μM
Bioavailability: 15%

Tuberculosis (TB) is an infectious disease, caused by the bacillus *Mycobacterium tuberculosis* (*Mtb*), and is the leading cause of death worldwide from a single infectious agent. According to the World Health Organization (WHO), approximately 10 million people acquired TB in 2018 and 1.2 million deaths occurred globally.[1] Treatments for drug-susceptible TB have been available for 60 years, with the current regimen comprising an initial two month intensive phase with four frontline drugs (isoniazid, rifampicin, ethambutol, and pyrazinamide), followed by a four month continuation phase using isoniazid and rifampicin. However, resistant strains have emerged over the years possibly as a result of poor patient compliance due to the extensive drug regimen, prolonged treatment time, socioeconomic factors, toxic effects, and the tendency to be asymptomatic before safe completion of the prescribed course.[2,3]

In the past 15 years, several new classes of anti-TB drugs have emerged in the developmental pipeline including three new agents. Bedaquiline and delamanid received accelerated regulatory approval in 2012 and 2014, respectively, and are being progressed into phase III clinical trials for the treatment of multidrug resistant TB (MDR-TB).[2−4] Most recently, pretomanid was approved as part of a six month, three-drug regimen consisting of bedaquiline, pretomanid, and linezolid

(BPaL) for the treatment of people with extensively drug resistant TB (XDR-TB).[5] Although there are a number of new chemical entities at various phases of clinical development,[6] the high attrition rate requires a continuous feed of new chemical matter into the drug discovery pipeline. The development of new TB treatments involves numerous challenges as the TB research community needs to focus on many aspects, e.g., shorter and simpler regimen, less side effects, effectiveness against drug resistant TB, reduced drug−drug interactions for human immunodeficiency virus (HIV)-coinfected patients, and affordable cost for patients in developing countries where the majority of TB cases exist.[7,8]

2-Aminoquinazolin-4(3*H*)-ones are derived from the quinazolinone class of compounds, which have been extensively explored in a wide range of therapeutic areas, whereas literature references on 2-aminoquinazolinones are
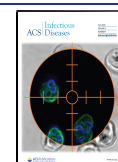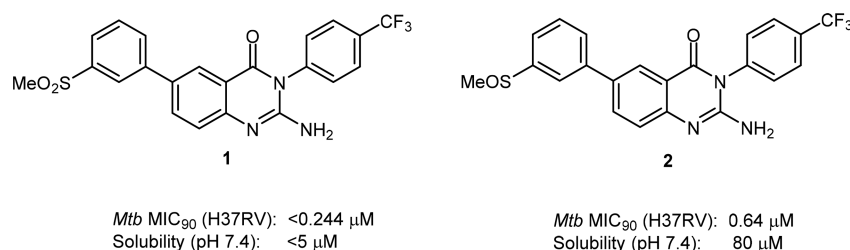
Figure 1. Identification of 2-aminoquinazolinones with *in vitro* antimycobacterial activity.

relatively scarce. Secondary and tertiary 2-amino analogues have been found to have pharmacological relevance, with examples of antifungal,[9] anti-inflammatory, anticancer,[10,11] antibacterial,[12,13] antihypertensive,[14] antidepressant,[15] and antimycobacterial activity.[16,17] On the other hand, primary 2-aminoquinazolinone derivatives have not yet been commercially developed but have shown a variety of biological activities as antimalarial,[18] antiviral,[19,20] and anticancer[21] agents. Although there is no known antimycobacterial activity, they appear as a valuable novel scaffold to explore as a potential anti-TB chemotype.

On the basis of structural similarity shared with a previously discovered antimalarial 2-aminopyridine series,[22] 2-aminoquinazolinones were synthesized for evaluation against the human malaria parasite *Plasmodium falciparum*. Subsequent phenotypic whole-cell cross-screening against *Mtb* identified the 2-aminoquinazolinone **1** as an attractive hit compound to follow up on despite its low solubility. During preliminary studies toward improving the solubility of **1**, the sulfone substituent was converted to the sulfoxide **2**, which displayed improved aqueous solubility while maintaining potency (Figure 1). As a result, medicinal chemistry efforts were subsequently pursued in order to explore the antimycobacterial potential of this 2-aminoquinazolinone series.

Herein, we present the synthesis, structure–activity relationship, *in vitro* absorption, distribution, metabolism, excretion, and toxicity (ADMET) properties, and *in vivo* pharmacokinetic (PK) properties of this series. *In vivo* efficacy and subsequent mechanistic studies are also presented.

RESULTS AND DISCUSSION

Chemistry. Structural modifications were explored around the aminoquinazolinone core with the aim of improving potency and aqueous solubility at pH 7.4. Four main points of diversity were established at positions 2, 3, 6, and 7 of the scaffold as indicated in Figure 2. R_1 and R_2 groups were
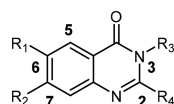
Figure 2. General structure of the quinazolinone core indicating modification sites.

investigated to identify appropriately substituted ring structures with various electronic, steric, and hydrophobicity properties. The addition of heteroatoms or water solubilizing groups was envisaged to reduce lipophilicity and, therefore, improve aqueous solubility. Additionally, the strategy of increasing sp^3 character through saturation of aromatic rings was employed to disrupt the crystal packing of molecules. The position of the substituent on the left-hand side (LHS) from

the 6- to the 7-position of the molecule was also explored to determine which of the LHS positions was optimal for activity. Modifications were also made to the 2-position to understand whether or not the 2-amino group was essential for potency.
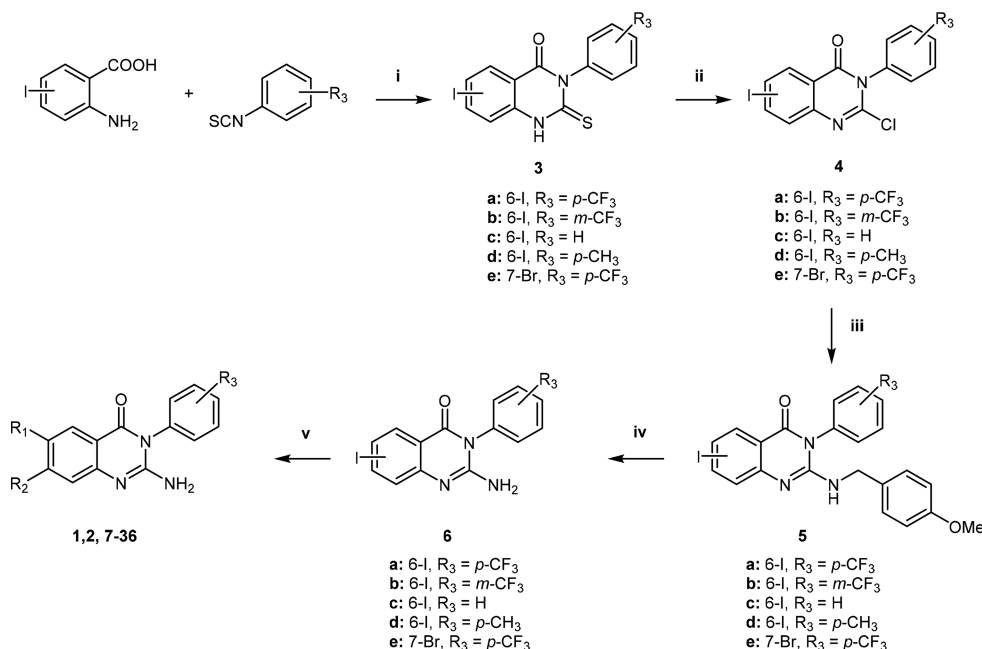
The synthesis of compounds **1**, **2**, and **7–36** was achieved following a relatively straightforward five-step synthetic route adapted from Leivers et al., starting with the commercially available 2-aminoiodobenzoic acid (Scheme 1).[19] Briefly, a cyclization reaction with the appropriately substituted phenyl isothiocyanate afforded intermediate **3**. Chlorination of the thioxo intermediate to **4** was obtained using phosphorus oxychloride (POCl$_3$) in the presence of phosphorus pentachloride (PCl$_5$). The 2-amino group was introduced via a 4-methoxybenzylamine intermediate (**5**) followed by deprotection of the PMB group to afford **6**. Finally, a Suzuki cross-coupling reaction with the appropriate boronic acids yielded the desired compounds **1**, **2**, and **7–36**.

The procedure to obtain the analogue without the 2-amino substituent was adapted from Güngör et al.[23] (Scheme 2). This approach involved refluxing 2-amino-5-iodobenzoic acid with 4-(trifluoromethyl)aniline in the presence of triethoxymethane to afford the iodo intermediate **37**. A subsequent Suzuki-coupling reaction with (3-(methylsulfonyl)phenyl)boronic acid yielded the desired derivative devoid of the 2-amino group **38**.

Modifications to the 2-amino substituent were achieved using a similar synthetic route to Scheme 1, whereby the appropriate amine was installed by substituting the chloro group of intermediate **4a** under basic conditions. Thereafter, the final target compounds **40–43** were obtained using the Suzuki-coupling conditions described previously (Scheme 3).

Lastly, compounds **47–58** were prepared using a modified synthetic route established by Lecoutey et al. to introduce structural diversity at the R$_3$ position (Scheme 4).[24] Initially, methyl 2-amino-5-bromobenzoate was reacted with ethoxycarbonyl isothiocyanate to form the isolated thioureido intermediate **44**. Thereafter, cyclization and simultaneous amide coupling with the appropriate amine using the coupling agent 1-ethyl-3-(3-dimethylaminopropyl)carbodiimide (EDCI) afforded intermediate **45**, which was deprotected to give **46**. Finally, the methylsulfinylphenyl moiety was installed via a Suzuki-coupling reaction to yield compounds **47–58**.

In Vitro Antimycobacterial Activity. Target compounds were initially evaluated for their *in vitro* antimycobacterial activity against the drug susceptible *Mtb* H37Rv strain, under replicating conditions using GASTE-Fe (glycerol–alanine–salts supplemented with Tween 80 and iron) culture media. The minimum inhibitory concentration (MIC$_{90}$) was read 14 days after incubation. Additionally, compounds were screened for *in vitro* cytotoxicity against a mammalian cell line, Chinese Hamster Ovarian (CHO). Initial structure–activity relationship (SAR) exploration was performed on the LHS with variations on the 6-position while keeping the 2-amino-

Scheme 1. General Synthetic Route for the Preparation of Compounds 1, 2, and 7−36[a]

3
a: 6-I, R$_3$ = p-CF$_3$
b: 6-I, R$_3$ = m-CF$_3$
c: 6-I, R$_3$ = H
d: 6-I, R$_3$ = p-CH$_3$
e: 7-Br, R$_3$ = p-CF$_3$

4
a: 6-I, R$_3$ = p-CF$_3$
b: 6-I, R$_3$ = m-CF$_3$
c: 6-I, R$_3$ = H
d: 6-I, R$_3$ = p-CH$_3$
e: 7-Br, R$_3$ = p-CF$_3$

1,2, 7-36

6
a: 6-I, R$_3$ = p-CF$_3$
b: 6-I, R$_3$ = m-CF$_3$
c: 6-I, R$_3$ = H
d: 6-I, R$_3$ = p-CH$_3$
e: 7-Br, R$_3$ = p-CF$_3$

5
a: 6-I, R$_3$ = p-CF$_3$
b: 6-I, R$_3$ = m-CF$_3$
c: 6-I, R$_3$ = H
d: 6-I, R$_3$ = p-CH$_3$
e: 7-Br, R$_3$ = p-CF$_3$

[a]Reagents and conditions: (i) dioxane, Et$_3$N, reflux (110 °C), 4 h; (ii) POCl$_3$, PCl$_5$, N$_2$, 110 °C, 14 h; (iii) DMF, 4-methoxybenzylamine, DIPEA, 80 °C, 4 h; (iv) TFA, reflux, 48 h or MW (110 °C) 20 min; (v) dioxane/water, R$_1$/R$_2$B(OH)$_2$, PdCl$_2$(PPh$_3$)$_2$, K$_2$CO$_3$, 80 °C, 1−5 h.

Scheme 2. Synthesis of Quinazolinone Analogue[a]

37

38
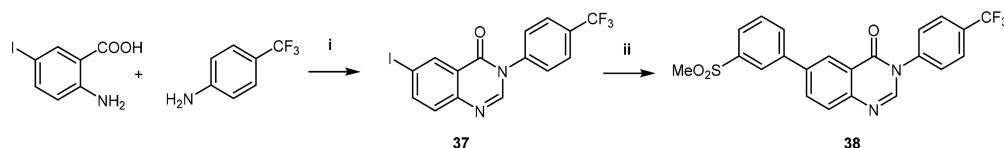
[a]Reagents and conditions: (i) triethoxymethane, dioxane, 100 °C, 16 h; (ii) dioxane, R$_1$B(OH)$_2$, PdCl$_2$(ddpf)$_2$-DCM, Cs$_2$CO$_3$, 90 °C, 5 h.[23]

Scheme 3. Synthetic Route Used to Access Core Modifications[a]


4a

39

40-43
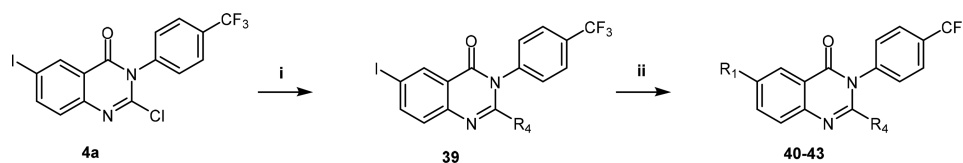
[a]Reagents and conditions: (i) relevant amine, DMF/THF, base, 80 °C, 3 h; (ii) dioxane/water, R$_1$B(OH)$_2$, PdCl$_2$(PPh$_3$)$_2$, K$_2$CO$_3$, 80 °C, 2 h.

quinazolinone core unchanged and the right-hand side (RHS) constant as a para-trifluoromethyl phenyl group (Table 1).

The R$_1$ phenyl group was first altered to explore the impact of various electronic effects and water solubilizing groups on activity. Changing the methyl sulfone in **1** to the more lipophilic cyclopropyl sulfone (**8**) led to a loss of activity, as did the introduction of a methyl group at the ortho-position of the biaryl moiety (**7**). Amide analogues (**9**, **10**, **11**) were generally equipotent to the sulfone derivative. Potency was also maintained when an aliphatic chain was extended off the amide functionality as in **13** and **14**. Various morpholino-type carboxamides were synthesized to improve aqueous solubility whereby the thiomorpholine analogue, **18**, was found to be highly potent (0.656 μM). Amides in the meta-position in combination with polar, ionizable groups, such as pyridyl groups **12** and **17** resulted in a 10- and 15-fold loss in activity, respectively. Transformation to the carboxylic acid group **20** was not tolerated (MIC$_{90}$ = 112 μM).

Replacements of the phenyl group by heterocycles were also investigated. While the unsubstituted pyridine (**22**) was equipotent to the frontrunner compounds **1** and **2**, the meta-substituted counterparts (**23** and **24**) displayed a loss in potency (MIC$_{90}$ >2 μM). Likewise, the pyrimidine analogue (**21**) was inactive. Exploration of electronic and lipophilic effects identified that electron withdrawing, lipophilic substituents (e.g., CF$_3$ and Cl groups as in **28** and **29**, respectively) were highly beneficial for potency, whereas electron donating groups (e.g., OMe, tBu, and NMe$_2$ as in **25**, **26**, and **27**, respectively) were not well-tolerated.

Subsequent SAR explorations focused on moving the LHS substituent from the 6- to the 7-position as well as varying the 2-amino moiety (Table 1). All 7-position derivatives (using side chains in the 6-position, which led to active compounds in order to have matched pairs) maintained potency (<2 μM), thus allowing variation on this position and broadening the SAR scope on the LHS. Thereafter, several analogues were

Scheme 4. General Route for the Synthesis of LHS Modifications[a]
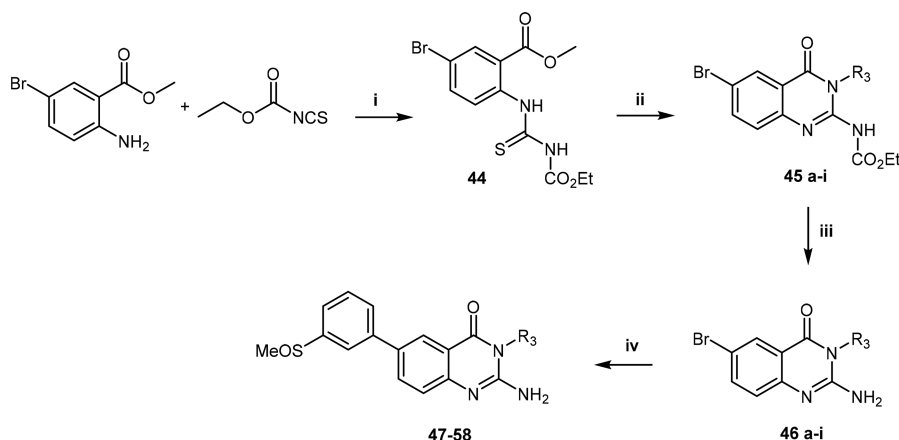
[a]Reagents and conditions: (i) acetonitrile, 25 °C, 10 min; (ii) DCM/DMF, EDCI, R_3NH_2, 25 °C, 18 h; (iii) TFA, microwave, 110 °C, 20 min; (iv) dioxane/water (4:1), $R_1B(OH)_2$, $PdCl_2(PPh_3)_2$, K_2CO_3, 80 °C, 5 h.

made to explore the scope of the 2-amino moiety while keeping either the phenyl sulfone or sulfoxide group at position 6. Removal of the 2-amino group as in compound **38** led to a 10-fold loss in potency (MIC_{90} = 2.96 μM) compared to the parent analogue **1**. Secondary (**40**) and tertiary (**42**) 2-amino analogues interestingly maintained some potency when the 6-position contained the sulfoxide substituent (MIC_{90} = 1.4 and 2.89 μM, respectively), whereas the sulfone counterparts (**41** and **43**) were inactive (MIC_{90} >125 μM). The majority of compounds in this series were found to be noncytotoxic except for the cyclopropyl sulfone (**8**), tertiary amide (**10**), and morpholino (**16**) substituted analogues, although cytotoxicity data always has to be evaluated critically when they are higher than the solubility data.

As far as the SAR exploration on the RHS is concerned, diverse groups were investigated to replace the trifluoromethyl substituent, while keeping the 2-aminoquinazolinone core unchanged and keeping the LHS group as a phenyl sulfoxide at position 6 constant, so that matched pairs could be compared (Table 2). Initially, the exploration of the substitution pattern around the ring highlighted that the CF_3 substituent exhibited optimal potency when at the para-position compared to the ortho-position (**34**) and meta-position (**48**). Solubility improvement strategies by adding a pyridyl group (**47**) or introducing a saturated ring (**57**) maintained moderate potency (MIC_{90} = 0.922 and 2.75 μM, respectively), whereas the addition of a benzylic methylene linker (**58**) led to a loss in potency. The replacement of the trifluoromethyl substituent by polar groups (SO_2Me, OH, OMe, CN) was detrimental to activity, while lipophilic substituents (F, Me) allowed moderate potency to be retained. The unsubstituted phenyl ring analogue (**35**) was not tolerated (MIC_{90} = 33 μM). Overall, the RHS SAR revealed that directly attached phenyl rings bearing lipophilic groups at the para-position were optimal for activity.
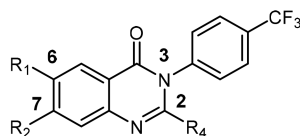
Physicochemical and *In Vitro* Microsomal Metabolic Stability Profiling. As mentioned previously, solubility was established as a critical parameter to optimize. Using the kinetic solubility assay, we aimed to achieve values >100 μM, but compounds with moderate solubility and potency were also progressed. To that effect, we looked at introducing hydrophilic groups as well as reducing overall aromaticity and planarity of the molecules (Table 1). For the latter, a methyl

substituent was inserted at the ortho-position to the LHS sulfone, as exemplified by **7**, in order to disrupt the planarity of the biaryl scaffold. This resulted in a 10-fold improvement in solubility (53.3 μM) with moderate potency (4.22 μM). Generally, derivatives from the R_1 SAR displayed poor to moderate solubility, except for **13** and **14** for which the addition of the aliphatic amide substituents drastically improved solubility (168 and 192 μM, respectively). The addition of heteroatoms as in **22** and **23** did not lead to improvements in solubility, except when the heterocycle contained an additional meta-substituent such as an amide (**12**) or methoxy (**24**) moiety (40 μM). Solubility for the morpholine-, thiomorpholine-, and piperazine-type derivatives (**16**, **18**, **19**) was moderately improved (46−56 μM).

With regards to microsomal metabolic stability, the LHS modifications led to generally metabolically stable derivatives across all species (human, rat, mouse). A few exceptions though include the morpholino derivative (**15**), thiomorpholine (**18**), pyridine (**22**), and the tertiary amine (**27**).

Modifications to the 2-position of the core scaffold maintained good metabolic stability, but no significant improvements were made in terms of solubility (Table 1). Removal of the 2-amino group decreased the solubility (**38** = <5 μM) of the sulfoxide derivative potentially due to the increase in lipophilicity (clogD = 4.25). The movement of the LHS group from position 6 to position 7 on the scaffold resulted in poor solubility, except for the primary amide derivative (**33**), which exhibited a 10-fold improvement compared to **9**.

RHS modifications were found to be the most favorable to improve aqueous solubility with five analogues (**34**, **58**, **36**, **53**, and **56**) exhibiting moderate to high solubility (>100 μM) (Table 2). The introduction of a pyridyl nitrogen (**47**) did not improve solubility as seen previously on the LHS; this could be due to the electron withdrawing nature of the trifluoromethyl substituent, which lowers the pK_a and reduces the ionizability of the nitrogen. The movement of the trifluoromethyl substituent from the para- to the meta-position was shown to be beneficial for solubility (164 μM), however, a reduction in metabolic stability was observed. Similarly, the incorporation of a benzyl linker improved solubility, albeit detrimental to metabolic stability. Variations of the trifluoromethyl substituent with hydrophilic, electron donating groups such

Table 1. SAR and *In Vitro* ADMET Data for LHS and Core Modifications

	R₁	R₂	R₄	MIC₉₀ GASTE-Fe (μM)	Cytotoxicity[a] μM (SI)	clogD[b]	Solubility pH 7.4[c] (μM)	Metabolic Stability H/R/M[d] (% Rem.)
1	*structure*	H	NH₂	<0.244	>100 (>400x)	3.29	<5	97/100/92
2	*structure*	H	NH₂	0.64	>100 (>156x)	3.56	80	88/-/-
7	*structure*	H	NH₂	4.22	>100 (>24x)	3.38	53	65/86/90
8	*structure*	H	NH₂	2.35	0.021 (0.01x)	3.56	66	85/98/97
9	*structure*	H	NH₂	<0.244	>100 (>400x)	3.10	<5	97/-/-
10	*structure*	H	NH₂	2.15	0.64 (0.3x)	3.14	46	85/86/89
11	*structure*	H	NH₂	0.78	96.3 (123x)	3.26	<5	98/100/100
12	*structure*	H	NH₂	9.22	ND	2.83	39	85/85/75
13	*structure*	H	NH₂	0.82	>50 (>61x)	3.14	168	82/40/56
14	*structure*	H	NH₂	1.03	>50 (>49x)	2.92	193	81/83/90
15	*structure*	H	NH₂	1.45	8.77 (6x)	3.82	<5	51/62/59
16	*structure*	H	NH₂	4.93	>50 (>10x)	3.44	56	71/77/78
17	*structure*	H	NH₂	83	ND	ND	ND	ND
18	*structure*	H	NH₂	0.656	>50 (>76x)	3.67	46	8/23/22
19	*structure*	H	NH₂	1.57	>50 (32x)	3.27	51	97/86/94
20	*structure*	H	NH₂	112	>100 (1x)	2.08	29	99/97/98
21	*structure*	H	NH₂	10	>100 (>10x)	3.03	40	94/-/-
22	*structure*	H	NH₂	0.625	>100 (>160x)	3.34	20	68/-/-
23	*structure*	H	NH₂	2.5	>100 (40x)	3.50	<5	87/-/-

Table 1. continued

	R_1	R_2	R_4	MIC$_{90}$ GASTE-Fe (μM)	Cytotoxicity[a] μM (SI)	clogD[b]	Solubility pH 7.4[c] (μM)	Metabolic Stability H/R/M[d] (% Rem.)
24	(structure)	H	NH$_2$	10	>100 (10x)	3.43	40	72/-/-
25	(structure)	H	NH$_2$	10	ND	ND	ND	ND
26	(structure)	H	NH$_2$	10	>100 (10x)	ND	ND	ND
27	(structure)	H	NH$_2$	2.5	>100 (40x)	3.76	20	37/-/-
28	(structure)	H	NH$_2$	0.75	>100 (130x)	4.01	40	88/-/-
29	(structure)	H	NH$_2$	0.675	ND	4.50	<5	73/-/-
30	H	(structure)	NH$_2$	1.39	>50 (>36x)	3.35	<5	99/99/99
31	H	(structure)	NH$_2$	1.32	>50 (>38x)	3.60	<5	98/73/78
32	H	(structure)	NH$_2$	0.80	>50 (>63x)	4.02	<5	95/89/82
33	H	(structure)	NH$_2$	1.22	ND	3.15	58	96/93/92
38	(structure)	H	H	2.96	ND	4.24	<5	ND
40	(structure)	H	(structure)	1.4	>50 (>36x)	3.62	64	89/90/87
41	(structure)	H	(structure)	>125	>50 (>0.4x)	3.34	<5	98/100/100
42	(structure)	H	(structure)	2.89	ND	3.61	<5	82/86/80
43	(structure)	H	(structure)	>125	ND	3.36	21.6	85/94/90
Rifampicin				0.0039				
Kanamycin				1.562				

[a]50% inhibitory concentration (IC$_{50}$) on Chinese Hamster Ovarian (CHO) cell lines. [b]clogD calculated using StarDrop. [c]Kinetic solubility assay at pH 7.4 using the HPLC method. [d]H/R/M: human/rat/mouse. SI: safety index. ND: Not determined.

as the methyl (**36**) and methoxy (**53**) moieties, resulted in improved solubility (172 and 128 μM, respectively), whereas electron withdrawing groups as in the monofluoro (**49**) and cyano (**54**) derivatives were relatively insoluble (37.8 and 16.3 μM). As expected, increasing sp^3 character through saturation of the aromatic ring led to improved solubility (**56** = 125 μM).

Despite multiple analogues being synthesized and exhibiting favorable *in vitro* properties, the two frontrunner compounds remained the best overall compounds in terms of combined potency, solubility, metabolic stability, and cytotoxicity properties. Therefore, compound **2** and its active metabolite, **1**, were selected for further *in vivo* PK studies.

In Vivo Pharmacokinetic Studies. *In vivo* PK studies were performed on compound **1** (sulfone) and compound **2** (sulfoxide) (Table 3). All studies and procedures were conducted with prior approval of the animal ethics committee of the University of Cape Town (approval numbers 013/028 and 014/028) in accordance with the South African National Standard (SANS 10386:008) for the Care and Use of Animals for Scientific Purposes and guidelines from the Department of Health. The sulfone **1** was poorly absorbed achieving a bioavailability of 18%. Compound **2** had much higher oral bioavailability and, notably, was converted *in vivo* to the sulfone (**1**). This resulted in a higher clearance for the sulfoxide **2** (21.8 vs 1.3 mL/min/kg). Higher exposure of the sulfone was achieved when the sulfoxide was dosed and underwent metabolic conversion than when the sulfone was dosed directly (AUC 18430 vs 7249 min·μmol·L^{-1}) as indicated in Figure 3.

In Vivo Tolerability and Efficacy Studies. The high exposure of the sulfone **1** achieved by dosing the sulfoxide **2** suggested that the sulfoxide could be used for *in vivo* efficacy experiments. Compound **2** was therefore dosed orally at 200 mg/kg to determine the exposure of the compound at the efficacious dose and to confirm that the exposure would be maintained long enough for efficacy. The free concentrations of compound **2** and its sulfone metabolite **1** are represented in Figure 4.

The free exposure was maintained above the MIC$_{90}$ of compound **1** for more than 24 h, and this dose was therefore projected to give *in vivo* efficacy.

To test compound **2** for *in vivo* efficacy, we employed the BALB/c acute TB mouse infection model (see Supporting Information, Section 4.2). In this model, mice are infected by

Table 2. SAR and *in Vitro* ADMET Data for RHS Modifications
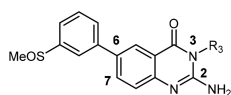
	R₃	MIC₉₀ GAST-Fe[a] (μM)	clogD[b]	Solubility[c] pH 7.4 (μM)	Met. Stab. H/R/M[d] (% Rem.)
2	*(4-CF₃-phenyl)*	0.64	3.56	80	88/-/-
34	*(3-CF₃-benzyl)*	14.8	3.55	164	50/58/51
35	*(benzyl)*	33.4	ND	ND	ND
36	*(4-methylbenzyl)*	3.09	2.92	172	99/68/71
47	*(pyridyl-CF₃)*	0.922	3.19	<5	93/99/93
48	*(2-CF₃-phenyl)*	>125	ND	ND	ND
49	*(4-F-benzyl)*	4.84	2.88	38	82/93/96
50	*(2-F-benzyl)*	67	ND	ND	ND
51	*(4-SO₂Me-phenyl)*	>125	ND	ND	ND
52	*(4-OH-benzyl)*	>125	ND	ND	ND
53	*(4-OMe-benzyl)*	6.75	2.67	128	100/103/99
54	*(4-CN-benzyl)*	9.28	2.73	16	92/98/91
55	*(3-CN-benzyl)*	43	ND	ND	ND
56	*(4,4-diF-cyclohexyl)*	45.7	3.36	125	95/81/83
57	*(CF₃-cyclohexyl)*	2.75	ND	ND	ND
58	*(4-CF₃-phenethyl)*	>31	3.62	104	52/61/69

[a]14 day readout against the H37Rv *Mtb*-GFP strain in GASTE-Fe media. [b]clogD calculated using StarDrop. [c]Kinetic solubility assay at pH 7.4 using the HPLC method. [d]H/R/M: human/rat/mouse. ND: Not determined.

Table 3. Pharmacokinetic Parameters for 1 and 2 after Intravenous and Oral Administration

parameter	1 iv	1 oral	2 iv	2 oral	1 as metabolite of 2 oral
dose (mg/kg)	5	20	5	20	20 of compound 2
C_{max} (μM)		5.98		3.54	10.4
T_{max} (h)		3		0.5	3
Vd (L/kg)	0.81		11.1		
apparent $t_{1/2}$ (h)	7.3		6.2		10.4
CL_{total} (mL·min⁻¹·kg⁻¹)	1.3		21.8		
$AUC_{0-\infty}$ (min·μmol·L⁻¹)	8589	7249	523	2152	18430
bioavailability (%)		18.4		93	

low dose aerosol, resulting in a mean of 2.86 $\log_{10}$ CFU *Mtb* Erdman-Lux in lungs 1 day following aerosol infection. The lung burdens increased to 4.16 $\log_{10}$ CFU at the start of treatment on day 7. Mice were then dosed once per day with **2** for 12 consecutive days by oral gavage in a 0.2 mL volume at 100 and 200 mg/kg. All mice completed the nonlethal acute TB efficacy trial as scheduled, and there was no evidence of compound tolerability issues. Three days following the last dose, the mean lung burdens were 6.51 $\log_{10}$ CFU for untreated mice compared to 5.72, 4.15, 7.84, and 7.75 $\log_{10}$ CFU for mice treated with rifampin at 10 mg/kg, ethambutol at 100 mg/kg, or **2** at 100 or 200 mg/kg, respectively. Thus, compound **2** was found to lack efficacy in the BALB/c acute infection model, showing higher overall lung burdens relative to the untreated controls. In contrast, rifampin at 10 mg/kg and ethambutol at 100 mg/kg reduced lung burdens as expected by 0.8 and 2.4 log, respectively.

On the basis of the *in vivo* PK and tolerability studies, the lack of *in vivo* efficacy is unlikely to be accounted for by low exposure and/or toxicity issues. In addition, plasma concentrations in infected mice at 1 and 24 h were comparable to those in healthy mice at the same time points (Table S1). This suggests that PK was similar between healthy and infected animals. Further investigation into the discrepancy between *in vitro* and *in vivo* results was therefore undertaken to understand the *in vitro*/*in vivo* disconnect.

Mechanistic Studies. Compound **2** was tested in biology triage assays to assess the activity against promiscuous targets. It did not show hypersensitivity against a cytochrome-*bd* oxidase knockout mutant strain (Δcyd GASTE-Fe MIC₉₀ = 2.5 μM), which is hypersusceptible to compounds that inhibit the QcrB-containing cytochrome *bc*1 complex, thereby eliminating QcrB as a potential target of **2**.[25,26] Additionally, **2** did not show a positive signal in two standard bioluminescence reporter assays: P*iniB*-LUX[27] detects modulation in *iniB* expression if compounds target *Mtb* cell-wall biosynthesis, and P*recA*-LUX[27] detects modulation in *recA* expression, an indicator of genotoxic compounds. On the basis of this initial triage process, the 2-aminoquinazolinone scaffold was identified as a hit series with a potential novel mechanism of action (MOA).

However, to further understand the discrepancy between *in vitro* and *in vivo* results, compound **2** was subsequently retested *in vitro* using different *Mtb* strains cultured in different media. As shown in Table 4, **2** was active against both H37Rv and Erdman *Mtb* strains when grown in media containing glycerol as the carbon source (7H9, glycerol, ADC, and Tween 80). In contrast to these observations, **2** lost activity against both strains when cultured in glycerol-free media (7H12, casitone, palmitic acid, BSA, catalase, and Tween 80).

Additional *in vitro* assays using glucose as the carbon source were performed on 15 other aminoquinazolinone analogues. In all cases, no activity was observed in the absence of glycerol in the culture medium, thus suggesting that the glycerol metabolism played a key role in effectively inhibiting *Mtb* growth. We therefore hypothesized that the *in vitro*/*in vivo* disconnect was due to the fact that glycerol was not used as a primary carbon source by *Mtb* in the mouse lungs, as has previously been observed.[28−30]

In order to test this hypothesis, MOA studies using spontaneous-resistant mutant generation combined with potential target identification using whole genome sequencing were performed with **2**. The spontaneous-resistant mutants
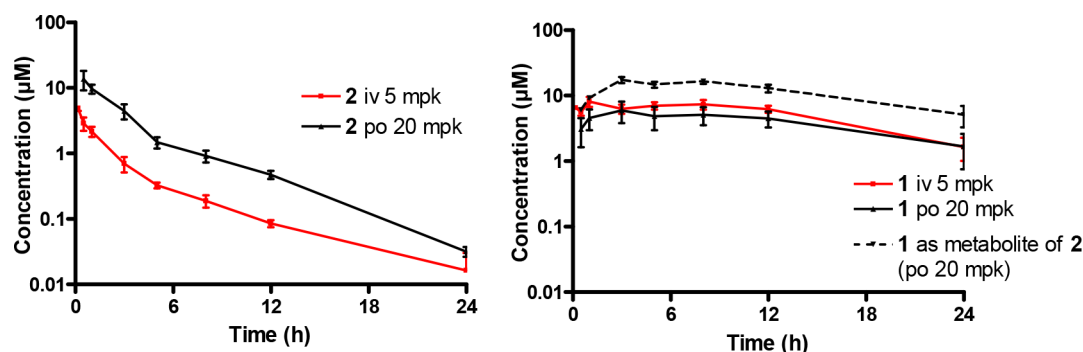
Figure 3. Concentration−time profiles for compound **2** (LHS graph) and its active metabolite **1** (RHS graph) at a 20 mg/kg oral dose (po) and 5 mg/kg intravenous (IV) dose.
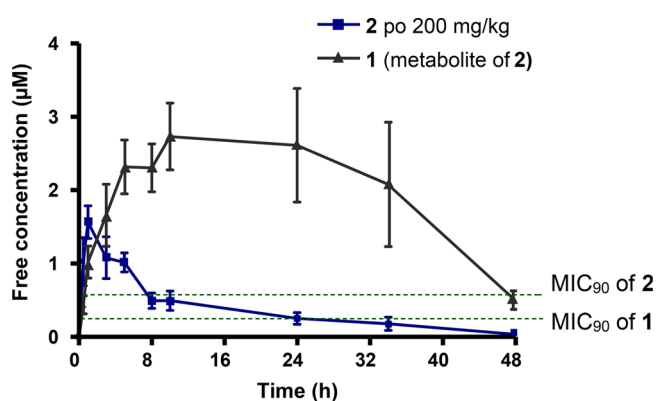
Figure 4. Free concentration−time profile of sulfoxide **2** and its sulfone metabolite **1** at 200 mg/kg dosed orally.

Table 4. *In Vitro* Antimycobacterial Activity of 2 in Different Assay Conditions

		MIC$_{90}$ (mg/L)		
strain	media	2	rifampin	isoniazid
Erdman	7H9 + glycerol + ADC + Tween 80	1	0.03	0.016
H37Rv	7H9 + glycerol + ADC + Tween 80	0.5	0.016	0.016
Erdman	7H12 + casitone + palmitic acid + BSA + catalase + Tween 80	>16	<0.008	0.016
H37Rv	7H12 + casitone + palmitic acid + BSA + catalase + Tween 80	>16	<0.008	0.016

were raised on Middlebrook 7H10 containing glycerol and OCDC (oleic acid, casitone, dextrose, and catalse) using the *Mtb* H37Rv MA strain. The mutants arose with a mutation frequency of 5×10^{-7}. Random isolated colonies were picked, grown in compound free medium, and tested for MIC at a compound concentration range of 0.16−160 μM. This led to the isolation of six *Mtb* spontaneous mutants (MIC$_{90}$ of compound **2**, >160 μM) with full genome sequencing revealing single nucleotide polymorphisms (SNPs) mapping exclusively to glycerol metabolizing genes, specifically *glpK* and *glpD2*, as described in Table 5. The *GlpK* gene (Rv3696) encodes for glycerol kinase, which is the first committing enzyme for glycerol metabolism in most bacteria. The second metabolite in the glycerol dissimilation pathway is dihydroxyacetone phosphate (DHAP), which is formed from glycerol-3-

Table 5. Description of Mutations Obtained from Spontaneous -Resistant Mutant Generation

no.	MIC$_{90}$ of 2 (μM)	gene	mutation	descriptor
1	>160	*glpK*	SNP	T96M
2	>160	*glpK*	frameshift mutation	C insertion at a.a. 189
3	>160	*glpK*	frameshift mutation	C insertion at a.a. 189
4	>160	*glpD2*	SNP	F122V
5	>160	*glpD2*	SNP	F122L
6	>160	*glpD2*	SNP	F122L

phosphate (G3P) by the enzyme glycerol-3-phosphate dehydrogenase encoded by the *glpD1* and *glpD2* genes.[28]

Previous reports observed that frameshift mutations and SNPs in *glpK* were linked to resistance to *Mtb* growth inhibitors.[28−30] These studies showed that compounds with glycerol-specific activity promote the accumulation of G3P, resulting in the rapid depletion of adenosine triphosphate (ATP) utilized for phosphorylation of glycerol, ultimately leading to self-poisoning of *Mtb*.[28,29] The activity of these compounds was therefore found to be associated with the metabolism of glycerol contained in 7H9 media.[28−30] No such reports have, however, been observed for *glpD2* mutants related to *in vitro* drug screening.

All considered together, the results from the MOA studies suggest that the aminoquinazolinone series potentially exert its inhibitory effect by dysregulating the glycerol dissimilation pathway,[31] leading to the toxic accumulation of sugar phosphates such as G3P and DHAP in *Mtb*.[28] When glycerol is not used as a carbon source by *Mtb in vivo*, compounds with such MOA do not show efficacy in the mouse model.

These results highlight the importance of validating the relevance of *in vitro* assay conditions to reproduce the environment encountered by *Mtb* in the infected host.[28,30] The culture media currently used for sufficient *Mtb* growth were empirically devised several decades ago for optimal propagation of the bacterium *in vitro* and were not optimized for drug screening efforts. Consequently, these media were not developed to replicate the conditions encountered by *Mtb in vivo*, thus limiting the predictive value of the *in vitro* assays. There is no clear consensus thus far as to which *in vitro* methods best reflect the *in vivo* biology in order to effectively identify novel candidates that will inhibit *Mtb* growth *in vivo*.[28,29,32]

■ CONCLUSION

This study identified a new class of aminoquinazolinone compounds active against *Mtb* through phenotypic whole-cell assays. Although these compounds exhibited excellent *in vitro* potency and favorable pharmacological properties, they were found to be inactive in an BALB/c mouse acute TB infection model. The discrepancy between *in vitro* activity and *in vivo* efficacy was elucidated through retesting *in vitro* using different *Mtb* strains cultured in different media, which revealed that activity was only observed in media containing glycerol. This was supported by spontaneous-resistant mutant generation and whole genome sequencing studies, which revealed mutations mapping to glycerol metabolizing genes, suggesting a major difference in carbon metabolism between bacteria growing in standard TB culture medium containing glycerol compared to those found in TB-infected lungs.

■ METHODS

General Methods. All reagents and solvents were obtained from commercial sources and used as received. All dry solvents were obtained from an SP-1 standalone solvent purification system from LC Technology Solutions Inc. Reactions were monitored by thin layer chromatography (TLC) using Merck TLC silica gel 60 F_{254} aluminum-backed precoated plates and were visualized by ultraviolet light at 254 nm. Purification of compounds was carried out by either column chromatography on silica gel 60 (Fluka), particle size of 0.063−0.2 mm (70−230 mesh ASTM), as the stationary phase or by Waters' HPLC using an X-bridge C18 5 μm column (4.6 × 150 mm). Additional details are as follows: organic phase, 10 mM ammonium acetate (pH 3.7) in HPLC grade methanol; aqueous phase, 10 mM ammonium acetate (pH 3.7) in HPLC grade water; flow rate, 15.00 mL/min; detector, photodiode array (PDA). All target compounds and intermediates were characterized by ^{1}H NMR, ^{13}C NMR, and MS. NMR spectra were recorded on either a Varian Mercury-300 (^{1}H 300.1 MHz, ^{13}C 75.5 MHz) or Bruker-400 (^{1}H 400.2 MHz, ^{13}C 100.6 MHz) instrument using CDCl$_3$, MeOH-d_4, and DMSO-d_6 as solvents. The ^{1}H NMR data are reported as follows: chemical shift in parts per million (δ) downfield of tetramethylsilane (TMS), multiplicity (s = singlet, bs = broad singlet, d = doublet, t = triplet, q = quartet, dd = doublets of doublets, dt = triplets of doublets, and m = multiplet), coupling constant (Hz), and integrated value. The ^{13}C NMR spectra were measured with complete proton decoupling. LC−MS/MS analysis was performed using an Agilent 1260 Infinity Binary Pump, Agilent 1260 Infinity Diode Array Detector (DAD), Agilent 1290 Infinity Column Compartment, Agilent 1260 Infinity Standard Autosampler, and an Agilent 6120 Quadrupole (Single) MS with an APCI/ESI multimode ionization source. The purities were determined by Agilent LCMS/MS or Waters' HPLC using an X-bridge C18 5 μm column (4.6 × 150 mm). Additional details are as follows: organic phase, 10 mM ammonium acetate (pH 3.7) in HPLC grade methanol; aqueous phase, 10 mM ammonium acetate (pH 3.7) in HPLC grade water; flow rate, 1.20 mL/min; detector, photodiode array (PDA). The purities of all compounds were found to be >95%.

6-Iodo-2-thioxo-3-(4-(trifluoromethyl)phenyl)-2,3-dihydroquinazolin-4(1H)-one (3a). A solution of 2-amino-5-iodobenzoic acid (5 g, 19 mmol, 1 equiv) and 4-(trifluoromethyl)phenyl isothiocyanate (4 g, 20 mmol, 1.05

equiv) in anhydrous 1,4-dioxane (75 mL) was treated with triethylamine (4 mL, 28.5 mmol, 1.5 equiv). The solution was heated under reflux for 4 h and cooled to room temperature, and the solids that formed were filtered. The solids were resuspended in diethyl ether (Et$_2$O) and filtered again to afford a white solid (7.84 g, 92%); ^{1}H NMR (300 MHz, DMSO-d_6) δ 13.18 (s, 1H), 8.20 (d, J = 1.9 Hz, 1H), 8.10 (dd, J = 8.6, 2.0 Hz, 1H), 7.88 (d, J = 8.3 Hz, 2H), 7.56 (d, J = 8.1 Hz, 2H), 7.26 (d, J = 8.6 Hz, 1H); ^{13}C NMR (101 MHz, DMSO-d_6) δ 176.14, 159.02, 144.21, 143.32, 139.64, 135.69, 130.72 (2C), 126.60 (2C), 126.56, 118.77, 118.54, 88.18, 66.84. LC-MS (ESI): found m/z = 448.9 [M + H]$^+$, (calcd for C$_{15}$H$_8$F$_3$IN$_2$OS: 447.0); HPLC purity 99%.

2-Chloro-6-iodo-3-(4-(trifluoromethyl)phenyl)quinazolin-4(3H)-one (4a). PCl$_5$ (6.37 g, 30.63 mmol, 1.75 equiv) was added in one portion to a mixture of intermediate **3** (7.84 g, 17.5 mmol, 1 equiv) in POCl$_3$ (40 mL, 25 equiv) at room temperature. The mixture was stirred for 15 min at room temperature and was subsequently heated to 110 °C for 14 h under nitrogen. The reaction was cooled to room temperature, concentrated *in vacuo*, and then diluted with ethyl acetate to be added portionwise to stirred ice-saturated sodium bicarbonate and stirred until all solids dissolved. The organic layer was then separated, washed with brine, dried over magnesium sulfate (Mg$_2$SO$_4$), and concentrated under reduced pressure. The resulting residue was triturated in Et$_2$O and filtered to obtain an off-white solid (6.26 g, 79%); ^{1}H NMR (300 MHz, DMSO-d_6) δ 8.39 (d, J = 1.8 Hz, 1H), 8.22 (dd, J = 8.5, 2.1 Hz, 1H), 7.99 (d, J = 8.3 Hz, 2H), 7.81 (d, J = 8.2 Hz, 2H), 7.52 (d, J = 8.7 Hz, 1H); ^{13}C NMR (101 MHz, DMSO-d_6) δ 150.20, 143.82, 139.91, 135.86, 135.42, 130.71 (2C), 130.44, 129.22, 127.13 (2C), 126.41, 118.23, 116.99, 85.69. LC-MS (ESI): found m/z = 450.9 [M + H]$^+$, (calcd for C$_{15}$H$_7$ClF$_3$IN$_2$O: 449.9); HPLC purity 90%.

6-Iodo-2-((4-methoxybenzyl)amino)-3-(4-(trifluoromethyl)phenyl)quinazolin-4(3H)-one (5a). 4-Methoxybenzylamine (2.36 mL, 18 mmol, 1.3 equiv) and *N,N*-diisopropylethylamine (DIPEA) (4.84 mL, 27.8 mmol, 2 equiv) were dissolved in DMF (45 mL), and the appropriate intermediate **4a** (6.26 g, 13.9 mmol, 1.0 equiv) was added portionwise. The reaction was stirred for 4 h at 80 °C and allowed to cool to room temperature. The solvent was concentrated under reduced pressure and diluted with EtOAc. The organic phase was washed with 5% lithium chloride (3 × 20 mL) and brine (20 mL), dried over Mg$_2$SO$_4$, and concentrated *in vacuo* to yield a brown solid (6.36 g, 83%); ^{1}H NMR (300 MHz, DMSO-d_6) δ 8.15 (d, J = 2.0 Hz, 1H), 7.97 (d, J = 8.3 Hz, 2H), 7.87 (dd, J = 8.6, 2.2 Hz, 1H), 7.67 (d, J = 8.1 Hz, 2H), 7.24 (d, J = 8.7 Hz, 2H), 7.11 (d, J = 8.7 Hz, 1H), 6.85 (d, J = 8.7 Hz, 2H), 6.68 (t, J = 5.9 Hz, 1H), 4.44 (d, J = 5.9 Hz, 2H), 3.71 (s, 3H); ^{13}C NMR (101 MHz, DMSO-d_6) δ 161.00, 158.55, 150.59, 149.58, 143.08, 139.05, 134.95, 132.01, 130.97 (2C), 130.70, 130.14 (q, J = 32.0 Hz, 1C, <u>C</u>-CF$_3$), 128.88 (2C), 124.7 (q, J = 272.5 Hz, 1C, <u>C</u>F$_3$), 127.75 (2C), 127.60, 119.49, 114.00 (2C), 84.74, 44.18. LC-MS (ESI): found m/z = 552.0 [M + H]$^+$, (calcd for C$_{23}$H$_{17}$F$_3$IN$_3$O$_2$: 551.0); HPLC purity 96%.

2-Amino-6-iodo-3-(4-(trifluoromethyl)phenyl)quinazolin-4(3H)-one (6a). Intermediate **5a** (6.35 g, 11.5 mmol, 1.0 equiv) was dissolved in TFA (56 mL, 64 equiv) and refluxed at 80 °C for 48 h. The reaction was cooled to room temperature, and the solvent was concentrated. The residue was resuspended in DCM and added portionwise to a stirred ice-

saturated sodium bicarbonate solution. The organic phase was separated; the aqueous phase was extracted with DCM, and the combined organic phases were diluted with Et$_2$O to a 1:1 ratio of DCM/Et$_2$O. The solids were filtered, washed with Et$_2$O, and dried under vacuum to afford an off-white solid (4.34 g, 87%); ^{1}H NMR (300 MHz, DMSO-d_6) δ 8.14 (d, J = 2.0 Hz, 1H), 7.93 (d, J = 8.3 Hz, 2H), 7.87 (dd, J = 8.7, 2.2 Hz, 1H), 7.63 (d, J = 8.1 Hz, 2H), 7.07 (d, J = 8.7 Hz, 1H), 6.60 (s, 2H); ^{13}C NMR (101 MHz, DMSO-d_6) δ 161.06, 152.21, 150.20, 143.04, 139.51, 135.01, 130.59 (2C), 130.03, 127.59, 127.55 (2C), 126.93, 119.24, 84.35. LC-MS (ESI): found m/z = 432.0 [M + H]$^+$, (calcd for C$_{15}$H$_9$F$_3$IN$_3$O: 431.0); HPLC purity 98%.

General Protocol for the Synthesis of Compounds 1, 2, and 7−36. To a solution of the relevant intermediate **6a−e** (1 equiv) and the appropriate arylboronic acid or ester (1.5 equiv) in anhydrous 1,4-dioxane (2 mL) flushed with nitrogen was added bis(triphenylphosphine) palladium(II) dichloride, PdCl$_2$(PPh$_3$)$_2$, (0.1 equiv); cesium carbonate or potassium carbonate (3 equiv) was dissolved in water (0.5 mL) and subsequently added to the reaction mixture. The solution was heated at 80 °C until TLC monitoring showed completion (1−5 h), allowed to cool to room temperature, and diluted with EtOAc to be filtered through Celite. The organic phase was washed with water (2 × 20 mL) and brine (20 mL), dried over Mg$_2$SO$_4$, and concentrated under reduced pressure. The resulting crude residue was purified by silica-gel flash chromatography eluting a gradient of either 0−100% EtOAc in hexane or 0−10% MeOH in DCM. Combined pure fractions were concentrated *in vacuo*, triturated with Et$_2$O, filtered, and dried under vacuum to give the relevant target compounds.

2-Amino-6-(3-(methylsulfonyl)phenyl)-3-(4-(trifluoromethyl)phenyl)quinazolin-4(3H)-one (1). Yield 77%. ^{1}H NMR (400 MHz, DMSO-d_6) δ 8.22 (d, J = 2.1 Hz, 1H), 8.18 (t, J = 1.7 Hz, 1H), 8.11 (ddd, J = 7.8, 1.8, 1.1 Hz, 1H), 8.09 (dd, J = 8.6, 2.4 Hz, 1H), 7.94 (d, J = 8.3 Hz, 2H), 7.88 (ddd, J = 7.8, 1.8, 1.0 Hz, 1H), 7.73 (t, J = 7.8 Hz, 1H), 7.65 (d, J = 8.1 Hz, 2H), 7.37 (d, J = 8.4 Hz, 1H), 6.57 (br s, 2H), 3.29 (s, 3H); ^{13}C NMR (101 MHz, DMSO-d_6) δ 162.24, 152.18, 150.88, 142.21, 140.96, 139.69, 133.66, 131.86, 131.66, 130.64 (2C), 130.17 (q, J = 32.0 Hz, 1C, $\underline{C}$-CF$_3$), 127.61, 127.58 (2C), 125.83, 125.41, 124.96, 124.87, 124.54 (q, J = 272.5 Hz, 1C, $\underline{C}$F$_3$), 117.40, 43.95. LC-MS (ESI): found m/z = 460.1 [M + H]$^+$, (calcd for C$_{22}$H$_{16}$F$_3$N$_3$O$_3$S: 459.09); HPLC purity 98%.

2-Amino-6-(3-(methylsulfinyl)phenyl)-3-(4-(trifluoromethyl)phenyl)quinazolin-4(3H)-one (2). Yield 57%. ^{1}H NMR (400 MHz, DMSO-d_6) δ 8.20 (d, J = 2.2 Hz, 1H), 8.03 (dd, J = 8.6, 2.2 Hz, 1H), 7.98 (t, J = 2.2 Hz, 1H), 7.95 (d, J = 8.2 Hz, 2H), 7.86 (dt, J = 6.6, 2.2 Hz, 1H), 7.70−7.62 (m, 4H), 7.37 (d, J = 8.6 Hz, 1H), 6.55 (br s, 2H), 2.81 (s, 3H); ^{13}C NMR (101 MHz, DMSO-d_6) δ 162.28, 152.08, 150.68, 147.89, 140.82, 139.73, 133.64, 132.55, 130.66 (2C), 130.45, 130.14 (q, J = 32.0 Hz, 1C, $\underline{C}$-CF3), 128.86, 127.61, 127.57, 125.34, 124.75, 124.7 (q, J = 272.48 Hz, 1C, $\underline{C}$F3), 122.64, 121.49, 117.37, 43.74. LC-MS (ESI): found m/z = 444.1 [M + H]$^+$, (calcd for C$_{22}$H$_{16}$F$_3$N$_3$O$_2$S: 443.1); HPLC purity 99%.

6-Iodo-3-(4-(trifluoromethyl)phenyl)quinazolin-4(3H)-one (37). To a solution of 2-amino-5-iodobenzoic acid (330 mg, 1.25 mmol, 1 equiv) and 4-(trifluoromethyl)aniline (200 mg, 1.25 mmol, 1 equiv) in dioxane (30 mL) was added

triethoxymethane (2 g, 12.5 mmol, 10 equiv), and the resulting reaction mixture was heated in a sealed tube at a temperature of 100 °C. After 16 h, a precipitate is formed. The reaction mixture was cooled to room temperature at 25 °C; the precipitate was filtered, washed with Et$_2$O (10 mL), and dried to afford a light yellow solid (150 mg, 0.36 mmol, 29%). LC-MS (ESI): found m/z = 417.0 [M + H]$^+$, (calcd for C$_{15}$H$_8$F$_3$IN$_2$O: 416.0); HPLC purity 80%.

6-(3-(Methylsulfonyl)phenyl)-3-(4-(trifluoromethyl)-phenyl)quinazolin-4(3H)-one (38). 6-Iodo-3-(4-(trifluoromethyl)phenyl)quinazolin-4(3H)-one **37** (150 mg, 0.3 6 mmol, 1 equiv), (3-(methylsulfonyl)phenyl)boronic acid (78 mg, 0.39 mmol, 1.1 equiv), and PdCl$_2$(dppf) (30 mg, 0.041 mmol, 0.11 equiv) were dissolved in dioxane (3 mL). Thereafter, Cs$_2$CO$_3$ (230 mg, 0.706 mmol, 2 equiv) and water (0.3 mL) were added. The mixture was heated in a pressure tube to 85 °C for 2 h. The cooled mixture was diluted with 50 mL of a NaHCO$_3$ solution and extracted with EtOAc (2 × 50 mL). The organic phases were dried over Na$_2$SO$_4$ and evaporated. Flash chromatography eluting a gradient of 30−50% EtOAc in DCM and the evaporation of the product fractions yielded a white solid (80 mg, 50%). ^{1}H NMR (300 MHz, CDCl$_3$) δ (ppm) 8.63 (1H, d, J = 3.0 Hz), 8.30−8.28 (1H, m), 8.18 (1H, s), 8.21 (1H, dd, J = 3.0 and 9.0 Hz), 8.04−7.99 (2H, m), 7.93 (1H, d, J = 9.0 Hz), 7.88 (2H, d, J = 9.0 Hz), 7.77−7.71 (1H, m), 7.64 (2H, d, J = 9.0 Hz), 3.16 (3H, s). LC-MS (ESI): found m/z = 445.1 [M + H]$^+$, (calcd for C$_{22}$H$_{15}$F$_3$N$_2$O$_3$S: 444.08); HPLC purity 100%.

6-Iodo-2-(methylamino)-3-(4-(trifluoromethyl)phenyl)-quinazolin-4(3H)-one (39a). 2-Chloro-6-iodo-3-(4-(trifluoromethyl)phenyl)quinazolin-4(3H)-one (intermediate **4a**) (200 mg, 0.44 mmol, 1.0 equiv) was dissolved in THF (2 mL), and a 33% solution of methylamine in ethanol was added; the mixture was heated in a pressure tube to 60 °C for 3 h. Once cooled, 10 mL of water was added and this mixture was extracted with ethyl acetate (2 × 50 mL). The organic layers were dried over Na$_2$SO$_4$ and evaporated to afford an oily residue (240 mg, 121%). ^{1}H NMR (300 MHz, CDCl$_3$) δ (ppm) 8.44 (1H, d, J = 3.0 Hz), 7.93 (1H, dd, J = 3.0 and 9.0 Hz), 7.92 (2H, d, J = 9.0 Hz), 7.49 (2H, J = 9.0 Hz), 7.46 (1H, d, J = 9.0 Hz), 3.13−3.07 (3H, m). LC-MS (ESI): found m/z = 446.0 [M + H]$^+$, (calcd for C$_{16}$H$_{11}$F$_3$IN$_3$O: 444.99).

General Procedure for the Synthesis of Compounds 40 and 41. Intermediate **39** (120 mg, 0.22 mmol, 1.0 equiv), the relevant boronic acid (56 mg, 0.28 mmol, 1.3 equiv), and PdCl$_2$(dppf) (20 mg, 0.027 mmol, 0.12 equiv) were dissolved in dioxane (2 mL). Thereafter, cesium carbonate (230 mg, 0.71 mmol, 3 equiv) and water (0.3 mL) were added. The mixture was heated in a pressure tube to 80 °C for 3.5 h. Once complete, the mixture was cooled, diluted with water, and extracted with EtOAc (2 × 50 mL). The organic layers were dried over Na$_2$SO$_4$ and evaporated. Flash chromatography eluting a gradient of 20−40% THF in DCM afforded the target compounds **40** and **41**.

2-(Methylamino)-6-(3-(methylsulfinyl)phenyl)-3-(4-(trifluoromethyl)phenyl)quinazolin-4(3H)-one (40). Yield 75%. ^{1}H NMR (300 MHz, CDCl$_3$) δ (ppm) 8.22 (1H, d, J = 3.0 Hz), 8.06 (1H, dd, J = 3.0 and 9.0 Hz), 8.00−7.94 (3H, m), 7.90−7.86 (1H, m), 7.70−7.68 (4H, m), 7.47 (1H, d, J = 9.0 Hz), 6.08−6.02 (1H, m), 2.81 (6H, "s"). LC-MS (ESI): found m/z = 458.1 [M + H]$^+$, (calcd for C$_{23}$H$_{18}$F$_3$N$_3$O$_2$S: 457.11); HPLC purity 99%.

2-(Methylamino)-6-(3-(methylsulfonyl)phenyl)-3-(4-(trifluoromethyl)phenyl)quinazolin-4(3H)-one (41). Yield 55%. ^{1}H NMR (300 MHz, CDCl$_3$) δ (ppm) 8.40 (1H, d, *J* = 3.0 hz), 8.24−8.22 (1H, m), 7.98−7.90 (5H, m), 7.72−7.65 (2H, m), 7.53 (2H, d, *J* = 9.0 Hz), 4.13 (1H, sb), 3.13 (3H, s), 3.08 (3H, d, *J* = 6.0 Hz). LC-MS (ESI): found *m/z* = 474.1 [M + H]$^+$, (calcd for C$_{23}$H$_{18}$F$_3$N$_3$O$_3$S: 473.10); HPLC purity 98%.

2-(Dimethylamino)-6-iodo-3-(4-(trifluoromethyl)phenyl)-quinazolin-4(3H)-one (39b). 2-Chloro-6-iodo-3-(4-(trifluoromethyl)phenyl)quinazolin-4(3H)-one (4a) (220 mg, 0.488 mmol, 1 equiv) was dissolved in DMF (5 mL); dimethylamine hydrochloride (350 mg, 4.8 mmol, 10 equiv), and 1 mL of triethylamine was added, and the mixture was then heated in a pressure tube to 80 °C for 3 h. To the cooled mixture was added 50 mL of water, and this mixture was extracted with ethyl acetate (2 × 50 mL). The organic layers were dried over Na$_2$SO$_4$ and evaporated to afford a yellow solid (270 mg, 120%). ^{1}H NMR (300 MHz, CDCl$_3$) δ (ppm) 8.36 (1H, d, *J* = 3.0 Hz), 7.83 (1H, dd, *J* = 3.0 and 9.0 Hz), 7.69 (2H, d, *J* = 9.0 Hz), 7.42 (2H, *J* = 9.0 Hz), 7.20 (1H, d, *J* = 9.0 Hz), 2.61 (6H, s). LC-MS (ESI): found *m/z* = 460.0 [M + H]$^+$, (calcd for C$_{17}$H$_{13}$F$_3$IN$_3$O: 459.0); HPLC purity 98%.

General Procedure for the Synthesis of 42 and 43. Intermediate 39b (135 mg, 0.29 mmol, 1 equiv), the corresponding boronic acid (56 mg, 0.28 mmol, 1 equiv), and PdCl$_2$(dppf) (20 mg, 0.027 mmol, 0.1 equiv) were dissolved in dioxane (2 mL). Thereafter, cesium carbonate (250 mg, 0.77 mmol, 3.0 equiv) and water (0.3 mL) were added. The mixture was heated in a pressure tube to 80 °C for 3.5 h. Once complete, the mixture was cooled, diluted with water, and extracted with EtOAc (2 × 50 mL). The organic layers were dried over Na$_2$SO$_4$ and evaporated. Flash chromatography eluting a gradient of 40−80% EtOAc in hexane afforded the desired final compounds 42 and 43.

2-(Dimethylamino)-6-(3-(methylsulfinyl)phenyl)-3-(4-(trifluoromethyl)phenyl)quinazolin-4(3H)-one (42). Yield 80%. ^{1}H NMR (300 MHz, CDCl$_3$) δ (ppm) 8.40 (1H, d, *J* = 3.0 Hz); 8.00 (1H, dd, *J* = 3.0 and 9.0 Hz); 7.97−7.93 (1H, m); 7.84−7.62 (7H, m); 7.56 (1H, d, *J* = 9.0 Hz); 2.81 (3H, s); 2.78 (6H, s). LC-MS (ESI): found *m/z* = 472.1 [M + H]$^+$, (calcd for C$_{24}$H$_{20}$F$_3$N$_3$O$_2$S: 471.12); HPLC purity 98%.

2-(Dimethylamino)-6-(3-(methylsulfonyl)phenyl)-3-(4-(trifluoromethyl)phenyl)quinazolin-4(3H)-one (43). Yield 88%. ^{1}H NMR (300 MHz, CDCl$_3$) δ (ppm) 8.41 (1H, d, *J* = 3.0 hz), 8.24−8.22 (1H, m), 7.99−7.93 (3H, m), 7.81 (2H, d, *J* = 9.0 Hz), 7.72−7.65 (2H, m), 7.57 (2H, d, *J* = 9.0 Hz), 3.13 (3H, s), 2.75 (6H, s). LC-MS (ESI): found *m/z* = 488.1 [M + H]$^+$, (calcd for C$_{24}$H$_{20}$F$_3$N$_3$O$_3$S: 487.11); HPLC purity 98%.

Methyl 5-Bromo-2-(3-(ethoxycarbonyl)thioureido)-benzoate (44). Methyl 2-amino-5-bromobenzoate (3.58 g, 15.5 mmol, 1 equiv) was dissolved in acetonitrile (10 mL), and the yellow solution was treated with ethoxycarbonyl iso-thiocyanate (2.2 mL, 18.6 mmol, 1.2 equiv). After stirring for 10 min at room temperature, the precipitate that formed was filtered; the resulting mother liquor was concentrated, and solids were refiltered to afford methyl 5-bromo-2-(3-(ethoxycarbonyl)thioureido)benzoate as a white solid (5 g, 90%). ^{1}H NMR (400 MHz, chloroform-*d*) δ 12.61 (s, 1H), 8.47 (d, *J* = 8.9 Hz, 1H), 8.18 (s, 1H), 8.16 (d, *J* = 2.4 Hz, 1H), 7.68 (dd, *J* = 8.8, 2.5 Hz, 1H), 4.35 (q, *J* = 7.1 Hz, 2H), 3.97 (s, 3H), 1.37 (t, *J* = 7.1 Hz, 3H); ^{13}C NMR (101 MHz, chloroform-*d*) δ 178.10, 165.46, 151.67, 137.95, 135.35,

133.42, 127.86, 123.54, 118.74, 63.07, 52.81, 14.21. LC-MS (ESI): found *m/z* = 360.9, 362.9 (1:1) [M + H]$^+$, (calcd for C$_{12}$H$_{13}$BrN$_2$O$_4$S: 359.98); HPLC purity 99%.

Ethyl(6-bromo-4-oxo-3-(6-(trifluoromethyl)pyridin-3-yl)-3,4-dihydroquinazolin-2-yl)carbamate (45a). Intermediate 44 (4.94 g, 13.68 mmol, 1 equiv) was dissolved in DCM (60 mL), and 6-(trifluoromethyl)pyridin-3-amine (3.3 g, 20.5 mmol, 1.5 equiv) and EDCI (5.24 g, 27.36 mmol, 2 equiv) were successively added to the solution. The solution was allowed to stir at room temperature for 18 h. Thereafter, the organic layer was washed with 1% of 1 M HCl (2 × 20 mL), water, and brine (20 mL) and dried over magnesium sulfate. The solution was filtered, and the solvent was concentrated under reduced pressure to furnish a pale yellow solid (4.3 g, 69%). ^{1}H NMR (400 MHz, CDCl$_3$) δ 8.65 (d, *J* = 1.9 Hz, 1H), 8.34 (d, *J* = 2.2 Hz, 1H), 7.90−7.79 (m, 3H), 7.19 (d, *J* = 8.6 Hz, 1H), 4.13 (q, *J* = 7.1 Hz, 2H), 1.27 (t, *J* = 7.1 Hz, 3H). LC-MS (ESI): found *m/z* = 4570, 459.0 (1:1) [M + H]$^+$, (calcd for C$_{17}$H$_{12}$BrF$_3$N$_4$O$_3$: 456.0); HPLC purity 97%.

2-Amino-6-bromo-3-(6-(trifluoromethyl)pyridin-3-yl)-quinazolin-4(3H)-one (46a). The 2-carbamate-based inter-mediate 45a (4.17 g, 9.1 mmol, 1 equiv) was dissolved in TFA (14 mL, 20 equiv). This solution was heated under microwave conditions at 110 °C for 20 min. After cooling to room temperature and evaporating the solvent, the residue was dissolved in DCM/MeOH (1:1). Amberlyst A21 free base was then added to this solution; the mixture was stirred at ambient temperature for 45 min, followed by filtration and rinsing of the resin with MeOH. The filtrate was then concentrated under reduced pressure to give a residue that was triturated in Et$_2$O, filtered, and dried to afford an off-white solid (2.9 g, 64%). ^{1}H NMR (400 MHz, DMSO-*d$_6$*) δ 8.83 (d, *J* = 2.3 Hz, 1H), 8.22 (dd, *J* = 7.7, 2.3 Hz, 1H), 8.13 (d, *J* = 7.6 Hz, 1H), 7.97 (d, *J* = 2.4 Hz, 1H), 7.77 (dd, *J* = 8.8, 2.5 Hz, 1H), 7.23 (d, *J* = 8.7 Hz, 1H), 6.80 (br s, 2H). LC-MS (ESI): found *m/z* = 385.0, 387.0 (1:1) [M + H]$^+$, (calcd for C$_{14}$H$_8$BrF$_3$N$_4$O: 384.0); HPLC purity 99%.

2-Amino-6-(3-(methylsulfinyl)phenyl)-3-(6-(trifluoromethyl)pyridin-3-yl)quinazolin-4(3H)-one (47). (3-(Methylsulfinyl)phenyl)boronic acid (1.2 equiv) and the corresponding 2-amino-6-bromoquinazolinone-based inter-mediate 46a (1 equiv) were dissolved in DMF (5 mL). The mixture was flushed with nitrogen gas for about 10 min at room temperature, after which Pd(PPh$_3$)$_2$Cl$_2$ (0.05 equiv) and K$_2$CO$_3$ (3 equiv) were added successively, and the mixture was heated at 100 °C for 1 to 4 h. After cooling to room temperature, the mixture was diluted with EtOAc (10 mL) and water (30 mL) and then extracted with EtOAc (3 × 20 mL). The combined organic fractions were filtered through a pad of Celite, washed with 5% LiCl (3 × 30 mL) and brine (2 × 30 mL), and dried over anhydrous MgSO$_4$. The solvents were then removed *in vacuo* to yield a residue that was purified by flash chromatography eluting a gradient of 0−15% MeOH in DCM. Product fractions were combined, and the solvents were rotary evaporated to give a solid that was then triturated with Et$_2$O, filtered, or recrystallized in an appropriate solvent (ethanol was used in most cases) and dried to furnish the desired final target compounds. Yield 56%. ^{1}H NMR (400 MHz, DMSO-*d$_6$*) δ 8.86 (d, *J* = 2.3 Hz, 1H), 8.25 (dd, *J* = 8.3, 2.3 Hz, 1H), 8.22 (d, *J* = 2.3 Hz, 1H), 8.14 (d, *J* = 8.3 Hz, 1H), 8.05 (dd, *J* = 8.6, 2.4 Hz, 1H), 7.98 (dd, *J* = 2.2, 1.2 Hz, 1H), 7.91−7.84 (m, 1H), 7.71−7.64 (m, 2H), 7.39 (d, *J* = 8.6 Hz, 1H), 6.78 (br s, 2H), 2.82 (s, 3H). LC-MS (ESI): found: *m/z*

= 445.1 $[M + H]^+$, (calcd for $C_{21}H_{15}F_3N_4O_2S$: 444.09); HPLC purity 99%.

ASSOCIATED CONTENT

Supporting Information

The Supporting Information is available free of charge at https://pubs.acs.org/doi/10.1021/acsinfecdis.0c00252.

Additional details of the synthetic protocols and characterization of all intermediates and final compounds and the procedures used for the *in vitro* biological assays, ADMET, and *in vivo* studies (PDF)

AUTHOR INFORMATION

Corresponding Author

Kelly Chibale − *Drug Discovery and Development Centre (H3D), Department of Chemistry, Institute of Infectious Disease and Molecular Medicine, and South African Medical Research Council Drug Discovery and Development Research Unit, Department of Chemistry, University of Cape Town, Rondebosch 7701, South Africa; Department of Chemistry, University of Cape Town, Rondebosch 7701, South Africa;* orcid.org/0000-0002-1327-4727; Phone: +27-21-6502553; Email: Kelly.Chibale@uct.ac.za; Fax: +27-21-6505195

Authors

Jessica N. Akester − *Drug Discovery and Development Centre (H3D), Department of Chemistry, University of Cape Town, Rondebosch 7701, South Africa*

Paul Njaria − *Department of Chemistry, University of Cape Town, Rondebosch 7701, South Africa*

Aloysius Nchinda − *Drug Discovery and Development Centre (H3D), Department of Chemistry, University of Cape Town, Rondebosch 7701, South Africa*

Claire Le Manach − *Drug Discovery and Development Centre (H3D), Department of Chemistry, University of Cape Town, Rondebosch 7701, South Africa*

[†]**Alissa Myrick** − *Drug Discovery and Development Centre (H3D), Department of Chemistry and Institute of Infectious Disease and Molecular Medicine, University of Cape Town, Rondebosch 7701, South Africa*

Vinayak Singh − *Drug Discovery and Development Centre (H3D), Department of Chemistry, Institute of Infectious Disease and Molecular Medicine, and South African Medical Research Council Drug Discovery and Development Research Unit, Department of Chemistry, University of Cape Town, Rondebosch 7701, South Africa;* orcid.org/0000-0001-9002-2489

Nina Lawrence − *H3D, Division of Clinical Pharmacology, Department of Medicine, University of Cape Town, Observatory 7925, South Africa*

Mathew Njoroge − *H3D, Division of Clinical Pharmacology, Department of Medicine, University of Cape Town, Observatory 7925, South Africa;* orcid.org/0000-0003-1276-2224

Dale Taylor − *H3D, Division of Clinical Pharmacology, Department of Medicine, University of Cape Town, Observatory 7925, South Africa*

Atica Moosa − *MRC/NHLS/UCT Molecular Mycobacteriology Research Unit, Department of Pathology, University of Cape Town, Rondebosch 7701, South Africa*

Anthony J. Smith − *Mycobacteria Research Laboratories, Department of Microbiology, Immunology, and Pathology,*

Colorado State University, Fort Collins, Colorado 80523, United States

Elizabeth J. Brooks − *Mycobacteria Research Laboratories, Department of Microbiology, Immunology, and Pathology, Colorado State University, Fort Collins, Colorado 80523, United States*

Anne J. Lenaerts − *Mycobacteria Research Laboratories, Department of Microbiology, Immunology, and Pathology, Colorado State University, Fort Collins, Colorado 80523, United States*

Gregory T. Robertson − *Mycobacteria Research Laboratories, Department of Microbiology, Immunology, and Pathology, Colorado State University, Fort Collins, Colorado 80523, United States*

Thomas R. Ioerger − *Department of Computer Science, Texas A&M University, College Station, Texas 77843-3112, United States*

Rudolf Mueller − *Drug Discovery and Development Centre (H3D), Department of Chemistry, University of Cape Town, Rondebosch 7701, South Africa*

Complete contact information is available at:
https://pubs.acs.org/10.1021/acsinfecdis.0c00252

Author Contributions

The manuscript was written through contributions of all authors. All authors have given approval to the final version of the manuscript.

Notes

The authors declare no competing financial interest.
[†]A. Myrick: Deceased.

ACKNOWLEDGMENTS

DEDICATION

This paper is dedicated to Alissa Myrick.

ABBREVIATIONS

TB, tuberculosis; *Mtb*, *Mycobacterium tuberculosis*; INH, isoniazid; RIF, rifampicin; MDR, multidrug resistant; EDC, *N*-(3-(dimethylamino)propyl)-*N*'-ethylcarbodiimide hydrochloride; ADMET, absorption, distribution, metabolism, excretion, and toxicity; HPLC, high-performance liquid chromatography; LC-MS, liquid chromatography−mass spectrometry; MIC_{90}, concentration of drug that inhibits growth of

90% of the bacterial population; PPB, plasma protein binding; SRM, spontaneous-resistant mutants; SAR, structure—activity relationship; PK, pharmacokinetics; WHO, World Health Organization; LHS, left-hand side; RHS, right-hand side; GASTE-Fe, glycerol—alanine—salts supplemented with Tween 80 and iron; AUC, area under curve; MOA, mechanism of action; SNP, single nucleotide polymorphism; G3P, glycerol-3-phosohate; ATP, adenosine triphosphate; DCM, dichloromethane; DMF, dimethylformamide; THF, tetrahydrofuran; TFA, trifluoracetic acid; TLC, thin layer chromatography; NMR, nuclear magnetic resonance

■ REFERENCES

(1) WHO (2019) *Global tuberculosis report 2019*, WHO, Geneva.

(2) Horsburgh, C. R., Barry, C. E., and Lange, C. (2015) Treatment of Tuberculosis. *N. Engl. J. Med.* 373, 2149−2160.

(3) Dover, L. G., and Coxon, G. D. (2011) Current Status and Research Strategies in Tuberculosis Drug Development. *J. Med. Chem.* 54, 6157−6165.

(4) Liu, B., Li, F., Zhou, T., Tang, X. Q., and Hu, G. W. (2018) Quinoline Derivatives with Potential Activity Against Multidrug-Resistant Tuberculosis. *J. Heterocycl. Chem.* 55, 1863−1873.

(5) TB Alliance (2019) *FDA Approves New Treatment for Highly Drug-Resistant Forms of Tuberculosis*, https://www.tballiance.org/news/fda-approves-new-treatment-highly-drug-resistant-forms-tuberculosis (accessed 2020-02-24).

(6) Working Group for New TB Drugs *Clinical Pipeline*, https://www.newtbdrugs.org/pipeline/clinical (accessed 2020-01-16).

(7) Barry, C. E., Boshoff, H. I., Dartois, V., Dick, T., Ehrt, S., Flynn, J., Schnappinger, D., Wilkinson, R. J., and Young, D. (2009) The Spectrum of Latent Tuberculosis: Rethinking the Biology and Intervention Strategies. *Nat. Rev. Microbiol.* 7, 845−855.

(8) Koul, A., Arnoult, E., Lounis, N., Guillemont, J., and Andries, K. (2011) The Challenge of New Drug Discovery for Tuberculosis. *Nature* 469, 483−490.

(9) El-Hashash, M. A., Elshahawi, M. M., Ragab, E. A., and Nagdy, S. (2015) Synthesis and Antifungal Activity of Novel Quinazolin-4(3H)-One Derivatives. *Synth. Commun.* 45, 2240−2250.

(10) Radwan, A. A., Alanazi, F. K., and Al-Dhfyan, A. (2013) Synthesis, and Docking Studies of Some Fused-Quinazolines and Quinazolines Carrying Biological Active Isatin Moiety as Cell-Cycle Inhibitors of Breast Cancer Cell Lines. *Drug Res. (Stuttgart, Ger.)* 63, 129−136.

(11) Rizza, P., Pellegrino, M., Caruso, A., Iacopetta, D., Sinicropi, M. S., Rault, S., Lancelot, J. C., El-Kashef, H., Lesnard, A., Rochais, C., Dallemagne, P., Saturnino, C., Giordano, F., Catalano, S., and Ando, S. (2016) 3-(Dipropylamino)-5-Hydroxybenzofuro[2,3-f]Quinazolin-1(2H)-One (DPA-HBFQ-1) Plays an Inhibitory Role on Breast Cancer Cell Growth and Progression. *Eur. J. Med. Chem.* 107, 275−287.

(12) Alanazi, A. M., Abdel-Aziz, A. A.-M., Shawer, T. Z., Ayyad, R. R., Al-Obaid, A. M., Al-Agamy, M. H. M., Maarouf, A. R., and El-Azab, A. S. (2016) Synthesis, Antitumor and Antimicrobial Activity of Some New 6-Methyl-3-Phenyl-4(3H)-Quinazolinone Analogues: In Silico Studies. *J. Enzyme Inhib. Med. Chem.* 31, 721−735.

(13) Azab, M. E., Kassab, E. A., El-Hashash, M. A., and Ali, R. S. (2009) Synthesis and Antibacterial Activity of Some New 4(3H)-Quinazolin-4-One Derivatives. *Phosphorus, Sulfur Silicon Relat. Elem.* 184, 610−625.

(14) Hess, H. J., Cronin, T. H., and Scriabine, A. (1968) Antihypertensive 2-Amino-4(3H)-Quinazolinones. *J. Med. Chem.* 11, 130−136.

(15) Gupta, C. M., Bhaduri, A. P., and Khanna, N. M. (1968) Drugs Acting on the Central Nervous System. Syntheses of Substituted Quinazolinones and Quinazolines and Triazepino- and Triazocino-quinazolinones. *J. Med. Chem.* 11, 392−395.

(16) Couturier, C., Lair, C., Pellet, A., Upton, A., Kaneko, T., Perron, C., Cogo, E., Menegotto, J., Bauer, A., Scheiper, B., Lagrange, S., and Bacqué, E. (2016) Identification and Optimization of a New Series of Anti-Tubercular Quinazolinones. *Bioorg. Med. Chem. Lett.* 26, 5290−5299.

(17) Alagarsamy, V., Anjana, G. V., Sulthana, M. T., Parthiban, P., and Solomon, V. R. (2016) Antimicrobial Activities of Some Synthesized 1-(3-(2-Methylphenyl)-4-Oxo-3H-Quinazolin-2-Yl-4-(Substituted)Thiosemicarbazide Derivatives. *Russ. J. Bioorg. Chem.* 42, 332−339.

(18) Jirgensons, A., Domraceva, I., Lapsa, I., Rasina, D., Jaudzems, K., and Otikovs, M. (2015) *Novel Substituted 2-Aminoquinazolin-4(3H)-One Derivatives as Malarial Aspartic Protease Inhibitors*, WO/2015/063544.

(19) Leivers, A. L., Tallant, M., Shotwell, J. B., Dickerson, S., Leivers, M. R., McDonald, O. B., Gobel, J., Creech, K. L., Strum, S. L., Mathis, A., Rogers, S., Moore, C. B., and Botyanszki, J. (2014) Discovery of Selective Small Molecule Type III Phosphatidylinositol 4-Kinase Alpha (PI4KIIIα) Inhibitors as Anti Hepatitis C (HCV) Agents. *J. Med. Chem.* 57, 2091−2106.

(20) Banka, A. L., Botyanszki, J., Duan, M., Leivers, M. R., Shotwell, J. B., Tallant, M. D., Dickerson, S. H., Tai, V. W.-F., Mcfadyen, R. B., Redman, A. M., Yu, J., Li, X., Garrido, D. M., Catalano, J. G., and Adjabeng, G. (2012) *Quinazolinone Derivatives as Antiviral Agents*, WO2012087938A1.

(21) Hughes, A. N., Rafi, I., Griffin, M. J., Calvert, A. H., Newell, D. R., Calvete, J. A., Johnston, A., Clendeninn, N., and Boddy, A. V. (1999) Phase I Studies with the Nonclassical Antifolate Nolatrexed Dihydrochloride (AG337, THYMITAQ) Administered Orally for 5 Days. *Clin. Cancer Res.* 5, 111−118.

(22) Younis, Y., Douelle, F., Feng, T.-S., Cabrera, D. G., Le Manach, C., Nchinda, A. T., Duffy, S., White, K. L., Shackleford, D. M., Morizzi, J., Mannila, J., Katneni, K., Bhamidipati, R., Zabiulla, K. M., Joseph, J. T., Bashyam, S., Waterson, D., Witty, M. J., Hardick, D., Wittlin, S., Avery, V., Charman, S. A., and Chibale, K. (2012) 3,5-Diaryl-2-Aminopyridines as a Novel Class of Orally Active Antimalarials Demonstrating Single Dose Cure in Mice and Clinical Candidate Potential. *J. Med. Chem.* 55, 3479−3487.

(23) Güngör, T., Chen, Y., Golla, R., Ma, Z., Corte, J. R., Northrop, J. P., Bin, Dickson, J. K., Stouch, T., Zhou, R., Johnson, S. E., Seethala, R., and Feyen, J. H. M. (2006) Synthesis and Characterization of 3-Arylquinazolinone and 3-Arylquinazolinethione Derivatives as Selective Estrogen Receptor Beta Modulators. *J. Med. Chem.* 49, 2440−2455.

(24) Lecoutey, C., Fossey, C., Rault, S., and Fabis, F. (2011) Efficient Room-Temperature One-Pot Synthesis of 2-Amino-3-Alkyl(3-Aryl)Quinazolin-4(3H)-Ones. *Eur. J. Org. Chem.* 2011, 2785−2788.

(25) Arora, K., Ochoa-Montaño, B., Tsang, P. S., Blundell, T. L., Dawes, S. S., Mizrahi, V., Bayliss, T., Mackenzie, C. J., Cleghorn, L. A. T., Ray, P. C., Wyatt, P. G., Uh, E., Lee, J., Barry, C. E., and Boshoff, H. I. (2014) Respiratory Flexibility in Response to Inhibition of Cytochrome c Oxidase in Mycobacterium Tuberculosis. *Antimicrob. Agents Chemother.* 58, 6962−6965.

(26) Moosa, A., Lamprecht, D. A., Arora, K., Barry, C. E., Boshoff, H. I. M., Ioerger, T. R., Steyn, A. J. C., Mizrahi, V., and Warner, D. F. (2017) Susceptibility of Mycobacterium Tuberculosis Cytochrome Bd Oxidase Mutants to Compounds Targeting the Terminal Respiratory Oxidase, Cytochrome C. *Antimicrob. Agents Chemother.* 61, No. e01338-17.

(27) Naran, K., Moosa, A., Barry, C. E., Boshoff, H. I. M., Mizrahi, V., and Warner, D. F. (2016) Bioluminescent Reporters for Rapid Mechanism of Action Assessment in Tuberculosis Drug Discovery. *Antimicrob. Agents Chemother.* 60, 6748−6757.

(28) Pethe, K., Sequeira, P. C., Agarwalla, S., Rhee, K., Kuhen, K., Phong, W. Y., Patel, V., Beer, D., Walker, J. R., Duraiswamy, J., Jiricek, J., Keller, T. H., Chatterjee, A., Tan, M. P., Ujjini, M., Rao, S. P. S., Camacho, L., Bifani, P., Mak, P. A., Ma, I., Barnes, S. W., Chen, Z., Plouffe, D., Thayalan, P., Ng, S. H., Au, M., Lee, B. H., Tan, B. H., Ravindran, S., Nanjundappa, M., Lin, X., Goh, A., Lakshminarayana, S. B., Shoen, C., Cynamon, M., Kreiswirth, B., Dartois, V., Peters, E. C.,

Glynne, R., Brenner, S., and Dick, T. A. (2010) Chemical Genetic Screen in Mycobacterium Tuberculosis Identifies Carbon-Source-Dependent Growth Inhibitors Devoid of in Vivo Efficacy. *Nat. Commun. 1*, 57.

(29) Stanley, S. A., Grant, S. S., Kawate, T., Iwase, N., Shimizu, M., Wivagg, C., Silvis, M., Kazyanskaya, E., Aquadro, J., Golas, A., Fitzgerald, M., Dai, H., Zhang, L., and Hung, D. T. (2012) Identification of Novel Inhibitors of M. Tuberculosis Growth Using Whole Cell Based High-Throughput Screening. *ACS Chem. Biol. 7*, 1377−1384.

(30) Manjunatha, U. H., and Smith, P. W. (2015) Perspective: Challenges and Opportunities in TB Drug Discovery from Phenotypic Screening. *Bioorg. Med. Chem. 23*, 5087−5097.

(31) Baughn, A. D., and Rhee, K. Y. (2014) Metabolomics of Central Carbon Metabolism in Mycobacterium Tuberculosis. *Micro-biol. Spectrum 2*, 1−16.

(32) Yuan, T., and Sampson, N. S. (2018) Hit Generation in TB Drug Discovery: From Genome to Granuloma. *Chem. Rev. 118*, 1887−1916.